Video Article

Micro/Nano-scale Strain Distribution Measurement from Sampling Moiré Fringes

Qinghua Wang[1], Shien Ri[1], Hiroshi Tsuda[1]

[1]Research Institute for Measurement and Analytical Instrumentation, National Institute of Advanced Industrial Science and Technology (AIST)

Correspondence to: Qinghua Wang at wang.qinghua@aist.go.jp

URL: https://www.jove.com/video/55739
DOI: doi:10.3791/55739

Keywords: Engineering, Issue 123, Deformation distribution, strain measurement, sampling moiré, image processing, optical method, micro/nano-scale, composite materials

Date Published: 5/23/2017

Citation: Wang, Q., Ri, S., Tsuda, H. Micro/Nano-scale Strain Distribution Measurement from Sampling Moiré Fringes. *J. Vis. Exp.* (123), e55739, doi:10.3791/55739 (2017).

Abstract

This work describes the measurement procedure and principles of a sampling moiré technique for full-field micro/nano-scale deformation measurements. The developed technique can be performed in two ways: using the reconstructed multiplication moiré method or the spatial phase-shifting sampling moiré method. When the specimen grid pitch is around 2 pixels, 2-pixel sampling moiré fringes are generated to reconstruct a multiplication moiré pattern for a deformation measurement. Both the displacement and strain sensitivities are twice as high as in the traditional scanning moiré method in the same wide field of view. When the specimen grid pitch is around or greater than 3 pixels, multi-pixel sampling moiré fringes are generated, and a spatial phase-shifting technique is combined for a full-field deformation measurement. The strain measurement accuracy is significantly improved, and automatic batch measurement is easily achievable. Both methods can measure the two-dimensional (2D) strain distributions from a single-shot grid image without rotating the specimen or scanning lines, as in traditional moiré techniques. As examples, the 2D displacement and strain distributions, including the shear strains of two carbon fiber-reinforced plastic specimens, were measured in three-point bending tests. The proposed technique is expected to play an important role in the non-destructive quantitative evaluations of mechanical properties, crack occurrences, and residual stresses of a variety of materials.

Video Link

The video component of this article can be found at https://www.jove.com/video/55739/

Introduction

Micro/nano-scale deformation measurements are vitally essential for evaluating the mechanical properties, instability behaviors, residual stresses, and crack occurrences of advanced materials. Since optical techniques are non-contact, full-field, and non-destructive, various optical methods have been developed for deformation measurement during the last few decades. In recent years, the micro/nano-scale deformation measurement techniques mainly include the moiré methods[1,2,3,4], geometric phase analysis (GPA)[5,6], Fourier transformation (FT), digital image correlation (DIC), and electronic speckle pattern interferometry (ESPI). Among these techniques, GPA and FT are not well suited for complex deformation measurements because multiple frequencies exist. The DIC method is simple but powerless against noise because the deformation carrier is random speckle. Finally, ESPI is strongly sensitive to vibration.

Among micro/nano-scale moiré methods, the most commonly used methods at present are the microscope scanning moiré methods, such as electron scanning moiré[7,8,9], laser scanning moiré[10,11], and atomic force microscope (AFM) moiré[12], and some microscope-based moiré methods, such as the digital/overlapping moiré[13,14,15] method and the multiplication/fractional moiré method[16,17]. The scanning moiré method has many advantages, such as a wide field of view, high resolution, and insensitivity to random noise. However, the traditional scanning moiré method is inconvenient for 2D strain measurements because it is necessary to rotate the sample stage or the scanning direction by 90° and to scan twice to generate moiré fringes in two directions[18]. Rotation and the dual scanning processes introduce rotation error and take a long time, seriously influencing the measurement accuracy of the 2D strain, especially for the shear strain. Although the temporal phase-shifting technique[19,20] can improve the deformation measurement accuracy, it requires time and a special phase-shift device unsuitable for dynamic tests.

The sampling moiré method[21,22] has a high accuracy in displacement measurements and is now mainly used for deflection measurements on bridges when automobiles pass. To extend the sampling moiré method to micro/nano-scale 2D strain measurements, a reconstructed multiplication moiré method has been newly developed[23] from 2-pixel sampling moiré fringes, in which the measurements are twice as sensitive and the wide field of view of the scanning moiré method is kept. Moreover, the spatial phase-shifting sampling moiré method is also developed from multi-pixel sampling moiré fringes, allowing for high-accuracy strain measurements. This protocol will introduce the detailed strain measurement procedure and is expected to help researchers and engineers learn how to measure deformation, improving the manufacturing processes of materials and products.

Protocol

1. Confirmation of the Micro/Nano-scale Grid on the Specimen

1. **Machining of the Specimen**
   1. Cut the specimen to the size required by the specific loading device used under a microscope (*e.g.,* 1 x 5 x 30 mm^3), making the surface to be observed 1.5x greater than the region of interest.
   2. Polish the specimen surface to be observed (*e.g.,* 1 x 30 mm^2), successively using coarse and fine sand paper on an automatic polishing machine (*e.g.,* use SiC foil #320 for 3 min and then #800 for 1 min at 150 rpm and 30 N). Clean the specimen using water after each polishing step.
   3. Polish the same specimen surface, successively using coarse and fine polishing solutions on the automatic polishing machine (*e.g.,* use DP-Spray P 15 µm for 5 min, P 1 µm for 8 min, and P 0.25 µm for 10 min at 150 rpm and 30 N). Clean the specimen using water after each polishing step.

2. **Fabrication of the Micro/Nano-scale Grid If No Periodic Pattern Exists on the Specimen**
   NOTE: This step can be omitted if a natural periodic pattern exists on the micro/nano scale on the specimen surface. Choose the grid fabrication method from the following: ultraviolet (UV) or heating nanoimprint lithography (NIL)[26], electron beam lithography (EBL)[2], and focused ion beam (FIB) milling[6].
   NOTE: The grid fabrication process is introduced here, with UV NIL as an example.
   1. Drop 2 mL of UV resist on the specimen surface using a pipette.
   2. Coat the resist on the specimen surface using a spin coater at 1,500 rpm for 60 s.
   3. Press a nanoimprint mold to the resist layer at a pressure of 0.2 MPa. Expose the resist to UV with a wavelength of 375 nm for 30 s.
   4. Separate the nanoimprint mold from the specimen surface.

3. **Observation of the Grid on the Specimen Using a Microscope**
   1. Coat a platinum or gold layer with a thickness of 3-10 nm on the grid surface using an ion coater (*e.g.,* coating for 30 s at 3 Pa with a sputtering current of 30 mA).
   2. Put the specimen under a laser scanning microscope (LSM)[23].
      NOTE: Other microscopes can also be used, such as a transmission electron microscope (TEM)[5], an atomic force microscope (AFM)[12], or a scanning electron microscope (SEM)[7].
   3. Adjust the focus and save one grid image using the microscope by clicking "Capture" and "File | Export | Image File" in the image recording software of the microscope.

4. **Calculation of the Grid Pitch (nm or µm) of the Specimen from the Grid Image**
   1. Calculate the average value of more than 10 grid pitches in the central area of the grid image to avoid the potential influence of the scanning or lens distortion.
      NOTE: The grid on the specimen can be saved for several days at room temperature.

2. Acquisition of Grid Images in the Loading Test

1. **Preparation of the Loading Test Under the Microscope**
   1. Fix the specimen to a loading device, such as a tensile, compressive, heating, or electrical loading device, under the microscope.
      NOTE: If the grid pitch is less than 20 nm, a TEM or AFM should be used. If the grid pitch is 20 nm to 10 µm, an SEM can be used. If the grid pitch is greater than 400 nm, an LSM can be used.
   2. Set the load speed (*e.g.,*0.01 mm/s) and the load or displacement incremental step (*e.g.,* 0.5 N/step or 0.024 mm/step) according to the specific requirements. Preset both the load and displacement to zero.
   3. Make the grid surface in the observation plane. Choose an area of interest under a low magnification by moving or rotating the sample stage of the microscope.
   4. Select an appropriate magnification by making the grid pitch in the image greater than 1.8× one pixel size.
      NOTE: Usually, it is better to make the grid pitch in the image greater than 2 pixels. The more pixels one grid pitch corresponds, the higher the accuracy of the deformation measurement, but the smaller the field of view of the measurement.

2. **Collection of Grid Images in the Loading Test**
   1. Save a grid image of the area of interest before loading by clicking "Capture" and "File | Export | Image File" in the image recording software of the microscope.
   2. Begin to load the specimen *in situ* onto the microscope by exerting the first load step (*e.g.,* 0.5 N or 0.024 mm) using the operating software of the loading device.
   3. Record a grid image of the area of interest after the first load step (*e.g.,* at 0.5 N or 0.024 mm) by clicking "Capture" and "File | Export | Image File" in the image recording software of the microscope. Ensure that the magnification and working distance of the microscope remain unchanged.
   4. Continue to load the specimen by exerting each load step using the loading device. Record the grid image after each load step until the specimen is broken or until a certain value is attained (*e.g.,* load 19 times and record 19 grid images at 1 N, 1.5 N, 2.0 N, …, 10 N, at intervals of 0.5 N; or at 0.048 mm, 0.072 mm, 0.096 mm, …, 0.48 mm, at intervals of 0.024 mm). Make sure that the magnification and working distance of the microscope remains unchanged.
      NOTE: The grid images can be saved for an arbitrarily long period of time.

3. Generation of Sampling Moiré Fringes before and after Deformation

1. **Estimation of Grid Pitches (pixel) in the Grid Images**
   1. Estimate the grid pitch (unit: pixel) in the grid image before loading by measuring the distance between the centers of two adjacent grid dots in an image processing software (*e.g.,* Microsoft Paint).
   2. Estimate the grid pitch in the grid image at the maximum load.

2. **Determination of Sampling Pitch (pixel)**
   1. Move to step 3.2.2 when the grid pitches before and after deformation are between 1.8 and 2.5 pixels. Skip to step 3.2.3 when the grid pitches before and after deformation are between 2.4 and 3.6 pixels. Skip to step 3.2.4 when the grid pitches before and after deformation are greater than 3.2 pixels.
   2. Set the sampling pitch to T = 2 pixels. Skip to step 3.3.
   3. Set the sampling pitch to T = 3 pixels. Skip to step 3.3.
   4. Set the sampling pitch T to a positive integer within 0.75x and 1.25x the grid pitches before and after deformation, determined from abundant simulation results[22].
      NOTE: If there are 2 positive integers that meet the requirements in steps 3.2.1 and 3.2.4, it is better to choose the greater integer as the sampling pitch. If there are 3 or more positive integers that meet the requirements, it is better to choose the middle integer, as long as it is a little bit greater than the sampling pitch.

3. **Generation of Sampling Moiré Fringes Before Deformation**
   1. Open the grid image before deformation. Assuming that the x direction is horizontally rightward, the y direction is vertically downward, and the coordinate (0, 0) is at the top-left corner, calculate the image width W in the x direction and the image height H in the y direction.
      NOTE: The y direction can also be defined as vertically upward.
   2. Move to step 3.3.3 to generate moiré fringes in the y direction. Skip to step 3.3.7 to generate moiré fringes in the x direction.
   3. Process the grid image to a grating image using a low-pass filter (LPF). For example, use an FT algorithm to suppress the grating, with a principal direction of x, where the principal direction is defined as the direction perpendicular to the grating lines. Set the filter size to be close to the grid pitch.
   4. Thin out the grid image by only extracting the gray values in several horizontal lines, with the spacing of the sampling pitch T ($T \geq 2$) from $y = k$ pixels (k = 0) (**Figure 1**) (*i.e.,* only keep the gray values in sampling lines of $y = k$ pixels, $y = k+T$ pixels, … , $y = k + iT$ pixels, where i is a positive integer). Make the coordinate of the last sampling line, $k + iT$, less than the image height H.
   5. Generate a sampling moiré pattern in the y direction by performing full-field intensity interpolation (linear or B-spline) of the image with horizontal sampling lines.
   6. Generate other T-1 sampling moiré patterns in the y direction by repeating steps 3.3.4 and 3.3.5 T-1 times by changing k at the incremental step of 1 pixel (*i.e.,* shifting the starting point of thinning out to $y = k$ pixels; k = 1, …, T-1).
   7. Use the same procedures in steps 3.3.3-3.3.6 to generate T-step spatial phase-shifting sampling moiré patterns in the x direction by changing x to y in step 3.3.3, changing the image height H to the image width W, and changing y to x in steps 3.3.4-3.3.6.
      NOTE: The sampling pitch in the x direction can be different from that in the y direction.

4. **Generation of Sampling Moiré Fringes After Deformation**
   1. Open all grid images at different loads. Suppose the number of grid images is N.
   2. Generate N groups of T-step spatial phase-shifting moiré fringes in the y direction by repeating steps 3.3.3-3.3.6 N times.
   3. Generate N groups of T-step spatial phase-shifting moiré fringes in the x direction by repeating step 3.3.7 N times.

4. Deformation Measurement of the Specimen in the Loading Test

1. **Determination of the Intensities of Moiré Fringes Before and After Deformation**
   1. Extract the intensities of the T-step moiré fringes before deformation in the y direction in steps 3.3.5 and 3.3.6; determine those moiré intensities in the x direction in step 3.3.7. Describe the T-step ($T \geq 2$) moiré intensities before deformation in the j ($j = x, y$) direction using the following equation[23]:
      $$I_{m,j}(k) = A\cos[2\pi y(\frac{1}{p_j} - \frac{1}{T}) + 2\pi\frac{k}{T}] + D \quad (k = 0, 1, T\text{-}1 \text{ pixel}, j = x, y) \quad (1)$$
      where p_j is the grid pitch before deformation in the j ($j = x, y$) direction, A is the modulated amplitude, and D includes the background and the higher-frequency intensities.
   2. Extract the intensities of the T-step moiré fringes after deformation in the y direction in step 3.4.2 and determine those moiré intensities in the x direction in step 3.4.3. Describe the T-step ($T \geq 2$) moiré intensities after deformation in the j ($j = x, y$) direction using the same equation as above (Equation 1) by changing $I_{m,j}(k)$, p_j, A, and D to $I'_{m,j}(k)$, p'_j, A', and D', respectively, where the superscript single quote means after deformation.
      NOTE: If the sampling pitch is $T \geq 3$ pixels, ignore this step and skip to step 4.3.

2.
   1. Reconstruct multiplication moiré fringes from the multiplicative interference between the two-step sampling moiré intensities (**Figure 1a**) before deformation using the following equation[23]
      $$I_{multi,j} = I_{m,j}(0)I_{m,j}(1) = -\frac{A^2}{2}\cos[4\pi y(\frac{1}{p_j} - \frac{1}{T})] - \frac{A^2}{2} + D^2 \quad (2)$$
      where $I_{multi,j}$ stands for the intensity of the reconstructed multiplication moiré fringes in the j ($j = x, y$) direction before deformation.

2. Process the reconstructed multiplication moiré fringes before deformation using the fringe centering technique[24]. Assign consecutive integers and half integers f_j = [1, 1.5, 2, 2.5, …] to the fringe orders at the center lines of the reconstructed multiplication moiré.
NOTE: If the multiplication moiré fringes are too dense, the fringe orders of the two-step sampling moiré can be determined first (*i.e.,* $f_j(0)$ = [1, 0, 2, 0, 3, 0, …] and $f_j(1)$ = [0, 1.5, 0, 2.5, 0, 3.5, …]). The fringe order of the multiplication moiré fringes will be $f_j = f_j(0) + f_j(1)$ = [1, 1.5, 2, 2.5, 3, 3.5, …]. The rigid-body displacement will not affect the strain result.
3. Measure the relative strain of the specimen before deformation relative to the sampling pitch using the following equations[23]

$$\varepsilon_{j\_rela} = \frac{\partial u_{j\_rela}}{\partial j} = \frac{\partial f_j T}{\partial j} \quad (f_j = [1,\ 1.5,\ 2,\ 2.5,\ \ldots],\ j = x, y) \text{ (3)}$$

$$\gamma_{xy\_rela} = \frac{\partial u_{x\_rela}}{\partial y} + \frac{\partial u_{y\_rela}}{\partial x} \text{ (4)}$$

where u_{j_rela} and ε_{j_rela} represent the relative displacement and the relative strain of the specimen before deformation in the j (j = x, y) direction, respectively, and γ_{xy_rela} expresses the relative shear strain before deformation.
4. Repeat steps 4.2.1-4.2.3 to determine the relative strains of the specimen after deformation in the x and y directions for N times, changing $I_{multi,j}$, $I_{m,j}(0)$, $I_{m,j}(1)$, p_j, A, D, u_{j_rela} (j = x, y), ε_{j_rela}, and γ_{xy_rela} in equations (2)-(4) to $I'_{multi,j}$, $I'_{m,j}(0)$, $I'_{m,j}(1)$, p'_j, A', D', u'_{j_rela} (j = x, y), ε'_{j_rela}, and γ'_{xy_rela}, respectively, where the superscript single quote means after deformation.
5. Determine the actual normal strain ε_j in the j (j = x, y) direction, which is the relative change of the grid pitch and the shear strain, γ_{xy}, which is the absolute variation of the grid angle of the specimen caused by the load from the relative strains before and after deformation[20].

$$\varepsilon_j = \frac{\varepsilon'_{j\_rela} - \varepsilon_{j\_rela}}{1 + \varepsilon_{j\_rela}} \quad (j = x,\ y) \text{ (5)}$$

$$\gamma_{xy} = \gamma'_{xy\_rela} - \gamma_{xy\_rela} \text{ (6)}$$

3. **Deformation Measurement When the Sampling Pitch is T ≥ 3 pixels**
1. Calculate the phase of the sampling moiré fringes in the j (j = x, y) direction before deformation when k = 0 (**Figure 1b**) using the spatial phase-shifting technique[21]

$$\varphi_{m,j} = \text{-arctan} \frac{\sum_{k=0}^{T-1} I_{m,j}(k) \sin(2\pi k / T)}{\sum_{k=0}^{T-1} I_{m,j}(k) \cos(2\pi k / T)} \quad (j = x,\ y) \text{ (7)}$$

2. Obtain the phase of the sampling moiré fringes in the j (j = x, y) direction after deformation when k =0 by replacing $\varphi_{m,j}$ and $I_{m,j}(k)$ in equation (7) with $\varphi'_{m,j}$ and $I'_{m,j}(k)$, respectively, where the superscript single quote means after deformation. Repeat N times for N loads.
NOTE: If there is too much random noise in the phase distributions in steps 4.3.1 and 4.3.2, a sin/cos filter[25] can be used to smooth the phases.
3. Determine the phase difference of the sampling moiré fringes in the j (j = x, y) direction before and after deformation (*i.e.*,$\Delta\varphi_{m,j}=\varphi'_{m,j}-\varphi_{m,j}$).
4. Measure the distributions of displacement u_j, normal strain ε_j in the j (j = x, y) direction, and the shear strain γ_{xy} of the specimen caused by the load. Use the following equations[6,21]

$$u_j = -\frac{p_j}{2\pi} \Delta\varphi_{m,j} \quad (j = x,\ y) \text{ (8)}$$

$$\varepsilon_j = \frac{\partial u_j}{\partial j} \quad (j = x,\ y) \text{ (9)}$$

$$\gamma_{xy} = \frac{\partial u_x}{\partial y} + \frac{\partial u_y}{\partial x} \text{ (10)}$$

NOTE: If there is too much noise in the strain distributions, an average smoothing filter can be used, with a filter size smaller than 2 grid pitches.

4. **Result Storage**
1. Save the data of the moiré fringes, phases (when the sampling pitch is T ≥3 pixels), displacements, and strains in the forms of images, such as .tif or .bmp files, and text, such as .txt or .csv files.

Representative Results

The 2D displacement and strain distributions of two carbon fiber-reinforced plastic (CFRP) specimens (#1 and #2) were measured according to the moiré formation principle[23] and the measurement process (**Figure 1**). The CFRP specimens were made up of 10-11 μm-diameter K13D carbon fibers and epoxy resins. The deformation of CFRP #1 was determined using the reconstructed multiplication moiré method from two-step sampling moiré fringes, and that of CFRP #2 was measured using the spatial phase-shifting sampling moiré method from three-step sampling moiré fringes.

A) Deformation Measurement of CFRP #1

The thickness, length, and width of CFRP #1 were 1 mm, 22 mm, and 4 mm, respectively (**Figure 2a**). The length direction of all fibers was perpendicular to the 1 × 22 mm^2 surface, which was polished using sand papers and polishing solutions. A grid with a pitch of 3.0 μm was fabricated on the polished surface using UV nanoimprint lithography (**Figure 2b**). A strain gauge was pasted on the bottom 4 × 22 mm^2 surface to monitor the greatest tensile strain.

A three-point bending test was carried out on CFRP #1 using a loading jig, with a support span of 16 mm, under a laser scanning microscope. The span-to-depth ratio was 16 according to the American Society for Testing and Materials (ASTM) standards. The grid images when the strain-gauge values were 0 and 0.00533 (**Figure 2b**) were recorded. The magnification of the objective lens of the microscope was 5×, and the scanning resolution was 1,024 x 1,024. The *x* direction is horizontally rightward and the *y* direction is vertically upward.

Since the grid pitches on CFRP #1 in both the *x* and *y* directions were around 2 pixels in the recorded image, the down-sampling pitches in the two directions were set to be T = 2 pixels for the deformation measurement. To avoid the potential influence of scanning distortion, a central area with size of 1.26 x 0.53 mm^2 was chosen as the area of interest. From 2-pixel down-sampling and equation (2), 2-step sampling moiré patterns and the reconstructed multiplication moiré pattern were generated after deformation (**Figure 2c**). Using equations (3) and (4), the deformation relative to the sampling pitch when the strain gauge value was 0.00533 was calculated. Similarly, the relative deformation when the strain gauge value was 0 was also obtained. Finally, the actual deformation distributions, including the 2D displacements (**Figure 2d**), the 2D normal strains, and the shear strain (**Figure 2e**), were measured using equations (5) and (6).

From the displacement distributions (**Figure 2d**), the *x*-direction displacement is positive at the upper-left and lower-right corners, but negative at the other two corners. The *y*-direction displacement is negative in the whole area and at a minimum in the central area. This agrees well with the deformation features of a bending specimen. From the strain distributions (**Figure 2e**), the upper area bears compressive strain in the *x* direction but tensile strain in the *y* direction, and the lower area bears tensile strain in the *x* direction but compressive strain in the *y* direction, demonstrating an interesting deformation characteristic. The shear strain is negative in the left area and positive in the right area, conforming to the bending property.

B) Deformation Measurement of CFRP #2

The thickness, length, and width of the laminated CFRP #2 were 1 mm, 30 mm and 5 mm, respectively (**Figure 3a**). There were 8 layers, and the thickness of each layer was 0.13 mm. The length direction of all fibers was perpendicular to the 1 x 30 mm^2 surface, which was polished using sand papers and polishing solutions. A grid with pitch of 3.7 μm was then fabricated on the polished surface using UV nanoimprint lithography (**Figure 3b**).

A three-point bending test was carried out using a loading jig, with support span of 16 mm, under a laser scanning microscope. The span-to-depth ratio was also 16. The grid image at the 0.2 N preload was first recorded. When the load was 10.8 N and the deflection was -200 μm, the deformed grid image was also recorded (**Figure 3b**). The magnification of the objective lens of the microscope was 5x, the imaging zoom was 120%, and the scanning resolution was 1,024 x 1,024 pixels. The *x* direction is horizontally rightward and the *y* direction is vertically upward.

Since the grid pitches on CFRP #2 in both the *x* and *y* directions were around 3 pixels in the recorded image, the down-sampling pitches in the two directions were set to be T = 3 pixels for the deformation measurement. To avoid the potential influence of the scanning distortion, a central area with a size of 1.15 x 0.49 mm^2 was chosen as the area of interest. Using the method described in step 4.3, the moiré phase distributions at 0.2 N and 10.8 N in both the *x* and *y* directions were obtained (**Figure 3c**). The distributions of the 2D in-plane displacements (**Figure 3d**), the 2D normal strains, and the shear strain (**Figure 3e**) were determined.

The displacement distribution (**Figure 3d**) features of CFRP #2 are similar to those of CFRP #1 (**Figure 2d**), except that the *y*-direction displacement is slightly different. The features of the *x*-direction strain and the shear strain of CFRP #2 (**Figure 3e**) are also similar to those of CFRP #1 (**Figure 2e**), agreeing with the deformation features of a bending specimen. However, the *y*-direction strain of CFRP #2 (**Figure 3e**) is different than that of CFRP #1 because CFRP #2 is a laminated specimen. Several layers can be observed from the distribution of the *y*-direction strain, which is almost negative in the whole area.

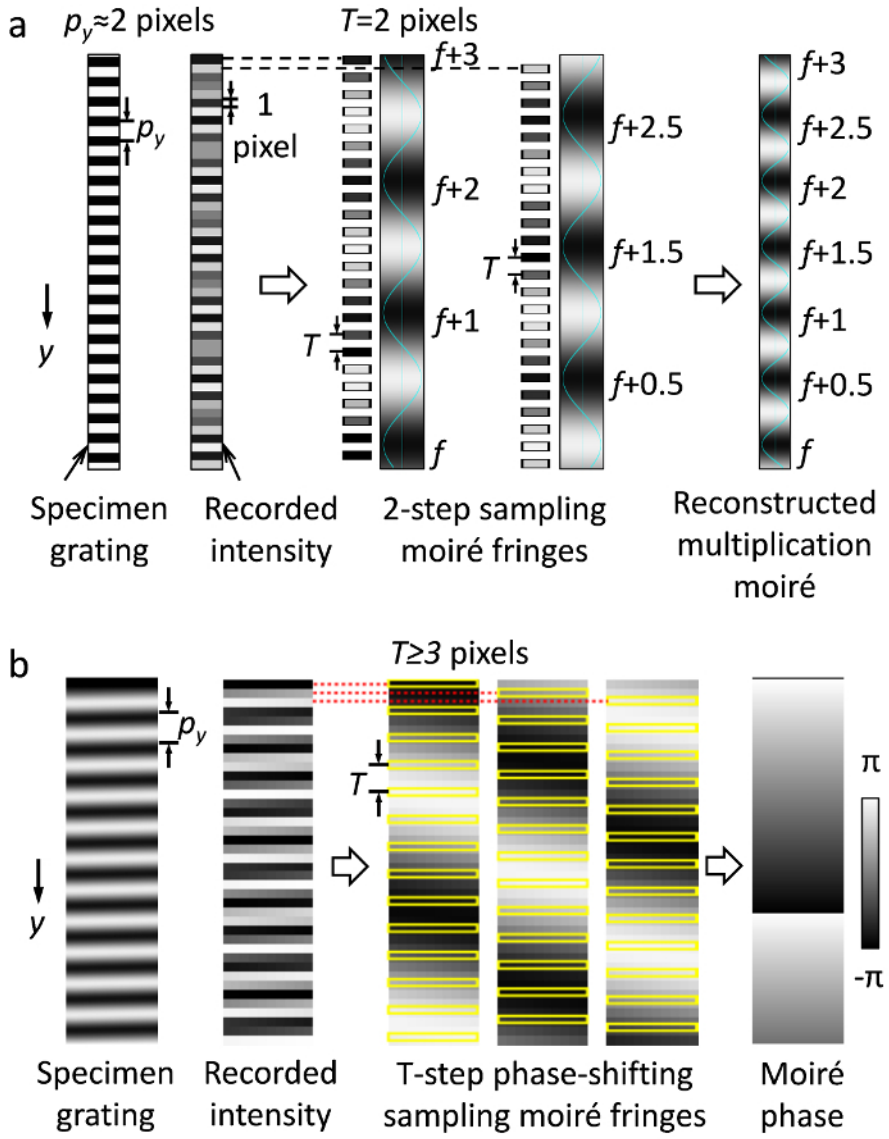

Figure 1: Sampling moiré formation principle and measurement process. (**a**) Generation principle of reconstructed moiré from 2-pixel sampling moiré fringes when the sampling pitch is T = 2 pixels. (**b**) Formation principle of multi-step phase-shifting sampling moiré fringes and the measurement process for the moiré phase when the sampling pitch is T ≥3 pixels. Please click here to view a larger version of this figure.

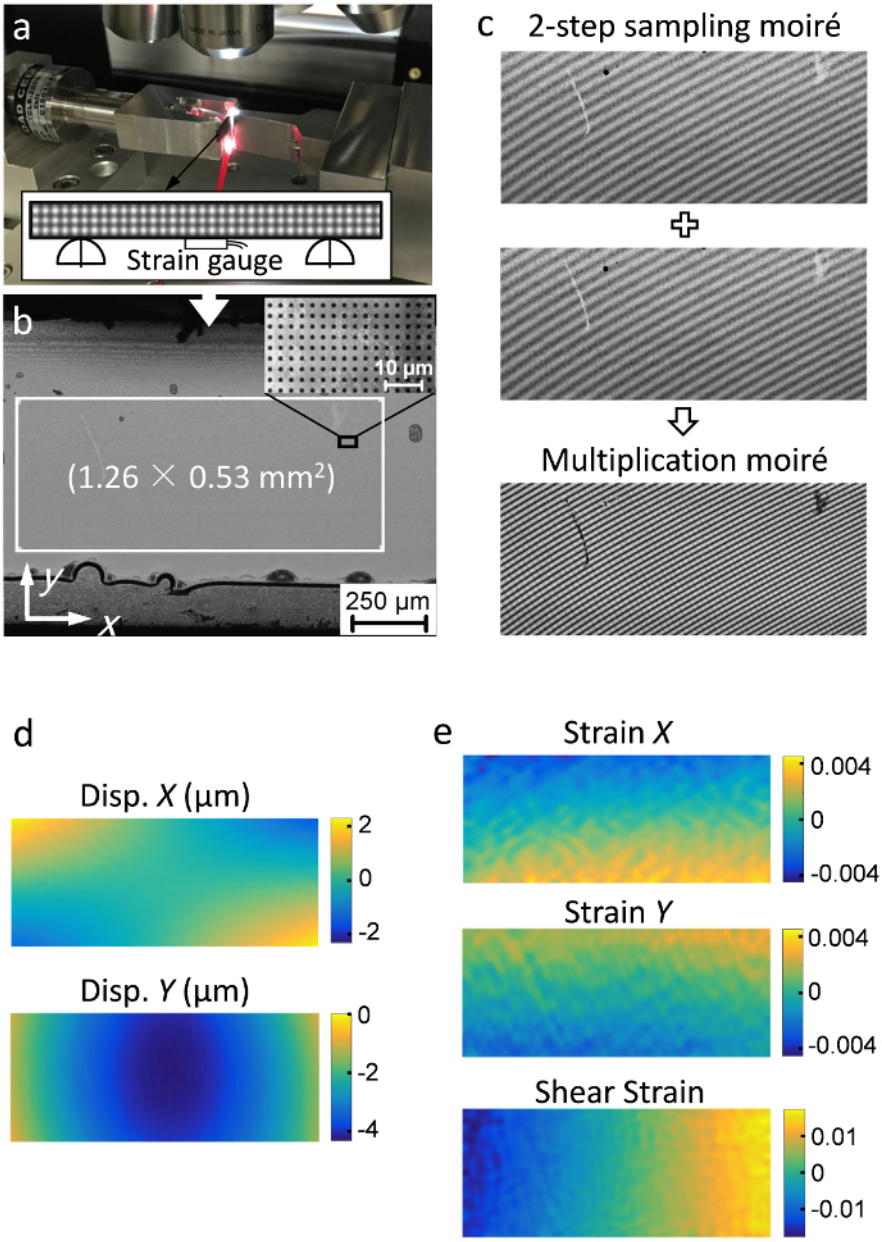

Figure 2: Deformation measurement results of CFRP #1. (**a**) Experimental setup of the three-point bending test under a laser microscope and the specimen diagram. (**b**) The observed surface of CFRP #1 with a micro grid. (**c**) Two-step sampling moiré patterns and the reconstructed multiplication moiré pattern when the strain gauge value was 0.00533. (**d**) The measured displacement distributions in the *x* and *y* directions. (**e**) The measured distributions of the *x* direction, *y* direction, and shear strains of CFRP #1. Please click here to view a larger version of this figure.

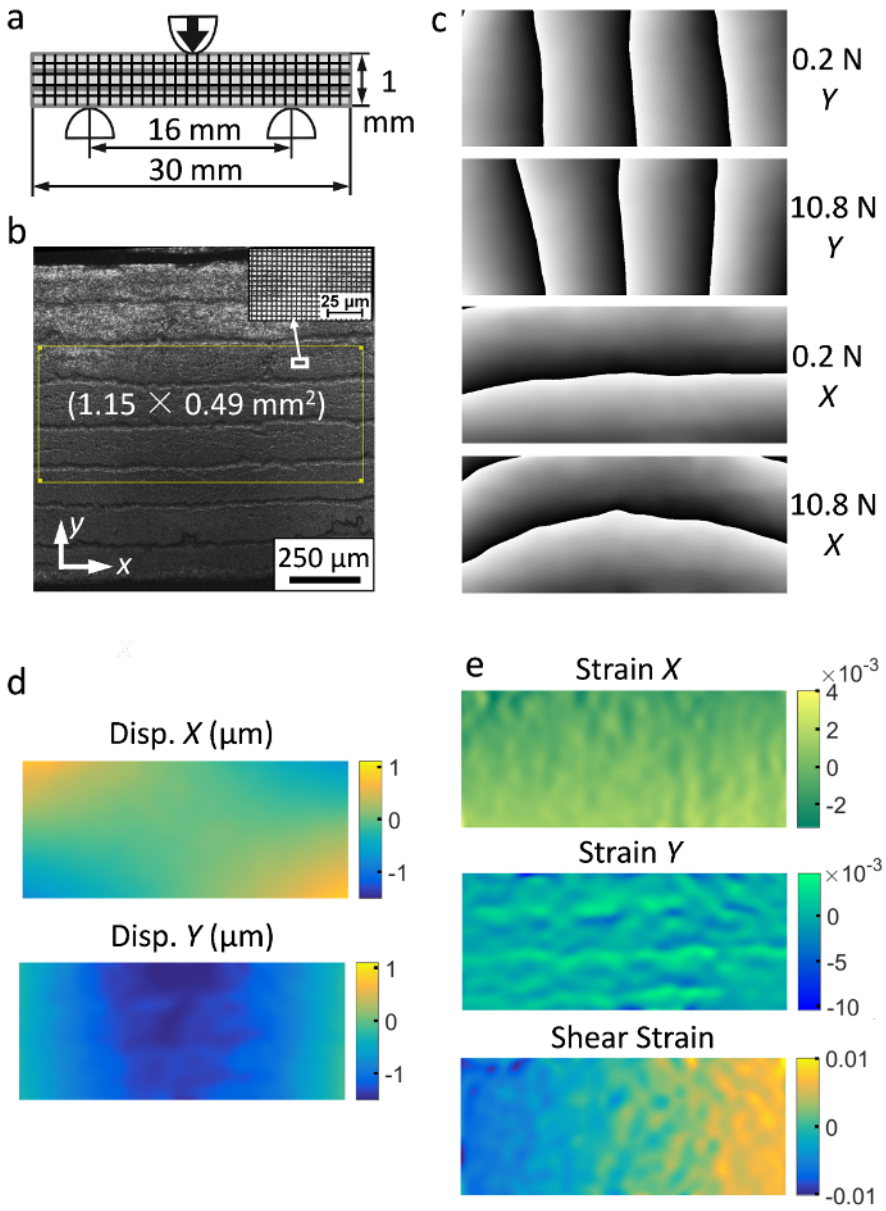

Figure 3: Deformation measurement results of laminated CFRP #2. (**a**) Diagram of the three-point bending test under a laser microscope. (**b**) The observed surface of CFRP #2 with a micro grid. (**c**) The wrapped phase (range: -π~π) distributions of the sampling moiré fringes at the 0.2 N preload and 10.8 N load in the *x* and *y* directions. (**d**) The measured displacement distributions in the *x* and *y* directions, where the deflection (-200 μm) in the *y* direction was not displayed. (**e**) The measured distributions of the *x* direction, *y* direction, and shear strains of CFRP #2. Please click here to view a larger version of this figure.

Discussion

In the described technique, one challenging step is the micro/nano-scale grid or grating (abbreviated as grid) fabrication[26] if no periodic pattern exists on the specimen. The grid pitch should be uniform before deformation because it is an important parameter for the deformation measurement. If the material is a metal, a metal alloy, or a ceramic, UV or heating nanoimprint lithography (NIL)[27], electron beam lithography (EBL)[2], focused ion beam (FIB) milling[6], or the grid duplicate method[26] can be used. If the material contains a weak polymer, EBL and FIB milling are not suggested. When a component of the material is not heat-resisting, heating NIL cannot be used. If the specimen is a thin film, the grid duplicate method is difficult to apply because it is not easy to separate the specimen.

The critical step for the strain measurement of the grid image before and after deformation using the proposed technique is the generation of sampling moiré fringes[22], the principle of which is different from the formation principle of conventional interference moiré fringes. To generate distinct sampling moiré fringes, a low-pass filter, such as an FT algorithm, is suggested to suppress unwanted lines or dots. If the sampling moiré fringes are indistinct after down-sampling (*i.e.,* thinning out the grid image) and linear-intensity interpolation, a smoothing filter, such as an

average filter, can be adopted before down-sampling. A second- or even third-order B-spline interpolation algorithm can be used for the intensity interpolation to generate distinct sampling moiré fringes.

Compared with the traditional moiré methods, the proposed sampling moiré technique for strain distribution measurement has the advantage of being a simple 2D strain measurement and having simple processing, high speed, high deformation sensitivity, and high measurement accuracy[23]. The 2D strain measurement can be easily performed without rotating the sample stage or the scanning lines of the microscope, which is necessary in conventional methods. In addition, dynamic deformation can be measured, as the required information is only a single-shot grid image at each load. This cannot be done with the temporal phase-shifting moiré method because several grid or moiré images are needed, along with time at each load.

Although the described technique allows for easy 2D strain measurements at the micro/nano scales, it has its own limitations[23], as does any other technique. The grid pitch in a recorded image should be greater than 1.8 pixels to generate 2-pixel or multi-pixel sampling moiré fringes. If the grid pitch in the image is around 2 pixels, the 2-pixel sampling moiré fringes can serve as the substitute for the microscope scanning moiré fringes, with the same field of view at the same magnification. However, if the grid pitch in an image is around 1 pixel at the highest scanning resolution of the microscope when distinct scanning moiré fringes are directly observable, sampling moiré fringes will be unable to form at the same magnification. Although sampling moiré fringes can be generated when increasing the microscope magnification, the field of view for the deformation measurement will decrease. Fortunately, the scanning resolutions of commercial microscopes are improving, and sampling moiré fringes can be generated in most cases. The higher the scanning resolution, the bigger the pixel number of one grid pitch, and the higher the strain measurement accuracy.

As opposed to the reconstructed multiplication moiré method from 2-pixel sampling moiré fringes, the spatial phase-shifting sampling moiré method from multi-pixel sampling moiré fringes has a higher processing speed and a higher measurement accuracy but a smaller field of view. The choice of method depends on the pixel number of the specimen grid pitch, or on the required measurement accuracy and field of view if the pixel number of the specimen grid pitch is controllable. Both methods are useful for taking nondestructive deformation measurements and making quantitative evaluations of mechanical properties, crack occurrence and growth, residual stresses, defect detection, structural characterization, *etc.*

Disclosures

The authors have nothing to disclose.

Acknowledgements

This work was supported by JSPS KAKENHI, grant numbers JP16K17988 and JP16K05996, and by the Cross-Ministerial Strategic Innovation Promotion Program, Unit D66, Innovative Measurement and Analysis for Structural Materials (SIP-IMASM), operated by the cabinet office. The authors are also grateful to Drs. Satoshi Kishimoto and Kimiyoshi Naito at NIMS for their CFRP material.

References

1. Weller, R., & Shepard, B. Displacement measurement by mechanical interferometry. *Proc. Soc. Exp. Stress Anal.* **6**(1), 35-38 (1948).
2. Kishimoto, S., Egashira, M., & Shinya, N. Microcreep deformation measurements by a moiré method using electron beam lithography and electron beam scan. *Opt. Eng.* **32**(3), 522-526 (1993).
3. Ifju, P., & Han, B. Recent applications of moiré interferometry. *Exp. Mech.* **50**(8), 1129-1147 (2010).
4. Zhang, H., Wu, C., Liu, Z., & Xie, H. A curved surface micro-moiré method and its application in evaluating curved surface residual stress. *Meas. Sci. Technol.* **25**(9), 095002 (2014).
5. Zhang, H., Liu, Z., Wen, H., Xie, H., & Liu, C. Subset geometric phase analysis method for deformation evaluation of HRTEM images. *Ultramicroscopy.* **171** 34-42 (2016).
6. Wang, Q., Kishimoto, S., Xie, H., Liu, Z., & Lou, X. In situ high temperature creep deformation of micro-structure with metal film wire on flexible membrane using geometric phase analysis. *Microelectron. Reliab.* **53**(4), 652-657 (2013).
7. Wang, Q., & Kishimoto, S. Simultaneous analysis of residual stress and stress intensity factor in a resist after UV-nanoimprint lithography based on electron moiré fringes. *J. Micromech. Microeng.* **22**(10), 105021 (2012).
8. Kishimoto, S., Wang, Q., Xie, H., & Zhao, Y. Study of the surface structure of butterfly wings using the scanning electron microscopic moiré method. *Appl. Opt.* **46**(28), 7026-7034 (2007).
9. Li, C., Liu, Z., Xie, H., & Wu, D. Novel 3D SEM Moiré method for micro height measurement. *Opt. Express.* **21**(13), 15734-15746 (2013).
10. Xie, H., Wang, Q., Kishimoto, S., & Dai, F. Characterization of planar periodic structure using inverse laser scanning confocal microscopy moiré method and its application in the structure of butterfly wing. *J. Appl. Phys.* **101**(10), 103511 (2007).
11. Tang, M., Xie, H., Wang, Q., & Zhu, J. Phase-shifting laser scanning confocal microscopy moiré method and its applications. *Meas. Sci. Technol.* **21**(5), 055110 (2010).
12. Xie, H, Kishimoto, S., Asundi, A., Boay, C.G., Shinya, N., Yu, J., & Ngoi, B.K. In-plane deformation measurement using the atomic force microscope moiré method. *Nanotechnology.* **11**(1), 24 (2000).
13. Xie, H., Liu, Z., Fang, D., Dai, F., Gao, H., & Zhao, Y. A study on the digital nano-moiré method and its phase shifting technique. *Meas. Sci. Technol.* **15**(9), 1716 (2004).
14. Wang, Q., Kishimoto, S., & Yamauchi, Y. Three-directional structural characterization of hexagonal packed nanoparticles by hexagonal digital moiré method. *Opt. Lett.* **37**(4), 548-550 (2012).
15. Liu, Z., Lou, X., & Gao, J. Deformation analysis of MEMS structures by modified digital moiré methods. *Opt. Lasers Eng.* **48**(11), 1067-1075 (2010).

16. Li, Y., Xie, H., Chen, P., & Zhang, Q. Theoretical analysis of moiré fringe multiplication under a scanning electron microscope. *Meas. Sci. Technol.* **22**(2), 025301 (2010).
17. Patorski, K., Wielgus, M., Ekielski, M., & Kaźmierczak, P. AFM nanomoiré technique with phase multiplication. *Meas. Sci. Technol.* **24**(3), 035402 (2013).
18. Wang, Q., Ri, S., Takashita, Y., & Ogihara, S. Full-field measurements of principal strains and orientations using moiré fringes. In: *Advancement of Optical Methods in Experimental Mechanics, Volume 3.* Yoshida, S., *et al.*, eds., Springer, Chapter 33, 251-259 (2017).
19. Wang, Z., & Han, B. Advanced iterative algorithm for phase extraction of randomly phase-shifted interferograms. *Opt. Lett.* **29**(14), 1671-1673 (2004).
20. Wang, Q., Xie, H., Hu, Z., Zhang, J., Sun, J., & Liu, G. Residual thermo-creep deformation of copper interconnects by phase-shifting SEM moiré method. *Appl. Mech. Mater.* **83**, 185-190 (2011).
21. Ri, S., Fujigaki, M., & Morimoto, Y. Sampling moiré method for accurate small deformation distribution measurement. *Exp. Mech.* **50**(4), 501-508 (2010).
22. Ri, S., & Muramatsu, T. Theoretical error analysis of the sampling moiré method and phase compensation methodology for single-shot phase analysis. *Appl. Opt.* **51**(16), 3214-3223 (2012).
23. Wang, Q., Ri, S., & Tsuda, H. Digital sampling Moiré as a substitute for microscope scanning Moiré for high-sensitivity and full-field deformation measurement at micron/nano scales. *Appl. Opt.* **55**(25), 6858-6865 (2016).
24. Dai, F., & Wang, Z. Automatic fringe patterns analysis using digital processing tehniques: I fringe center method. *Acta Photonica Sinica.* **28** 700-706 (1999).
25. Gutmann, B., & Weber, H. Phase-shifter calibration and error detection in phase-shifting applications: a new method. *Appl. Opt.* **37**(32), 7624-7631 (1998).
26. Wang, Q., Kishimoto, S., Tanaka, Y., & Kagawa, Y. Micro/submicro grating fabrication on metals for deformation measurement based on ultraviolet nanoimprint lithography. *Opt. Lasers Eng.* **51**(7), 944-948 (2013).
27. Min-Jin, T., Hui-Min, X., Yan-Jie, L., Xiao-Jun, L., & Dan, W. A new grating fabrication technique on metal films using UV-nanoimprint lithography. *Chin. Phys. Lett.* **29**(9), 098101 (2012).

